



Published in final edited form as:

Phys Rev Lett. 2009 April 10; 102(14): 148301. doi:10.1103/PhysRevLett.102.148301.

Amplification of Tension in Branched Macromolecules

Sergey V. Panyukov,

P. N. Lebedev Physics Institute, Russian Academy of Sciences, Moscow 117924, Russia

Sergei S. Sheiko, and

Department of Chemistry, University of North Carolina, Chapel Hill, North Carolina 27599-3290, USA

Michael Rubinstein

Department of Chemistry, University of North Carolina, Chapel Hill, North Carolina 27599-3290, USA

Abstract

We propose a method for the design of branched macromolecules that are capable of building up high tension (\sim nN) in their covalent bonds without applying an external force. The tension is self-generated due to repulsion between branches and depends on the molecular architecture leading to amplification and focusing of tension in specific bonds. The simplest architecture is a pom-pom composed of a linear spacer and two z -arm stars at its ends resulting in z -fold tension amplification. Adsorption of those macromolecules on a substrate results in further increase in tension as compared to molecules in solution.

Material properties, such as conductivity, color, and chemical reactivity change whenever molecules are under tension. Particularly strong effects are observed when the bond tension approaches the nano-Newton (nN) range, where covalent bonds typically rupture. This phenomenon is the subject of mechanochemistry [1] and mechanical biology [2–4]. Tension can be delivered to individual molecules using various micromanipulation techniques, such as atomic force microscopy, optical tweezers, and extensional flow [5–10]. However, controlling weak forces in single molecules is very challenging. Alternatively, molecules can be stretched by applying stress to bulk materials, such as polymer solutions, networks, and fibers [11–13]. In this case, the stress is distributed in a nonuniform way between many molecules. We propose a new method, which allows delivering high tension (\sim nN) to a large number of molecules in a controllable way without applying an external force. This method is based on intelligent molecular design which allows amplification of bond-tension from the pN to nN range. Recently, we have shown that nN tension is developed in brushlike macromolecules upon their adsorption to substrate [14]. In these experiments, the tension amplification is achieved due to adsorption-induced crowding of side chains. However, in solution, molecular brushes experience much lower tension (\sim 10 pN), which is experimentally undetectable. Here we show how to achieve nN bond tension in solution, which can be detected by available spectroscopic techniques and, thus, expands the range of practical applications of the designed molecules as sensors, drug delivery, and catalysts.

Two components are required for the construction of molecular tension amplifiers. The first component is a brushlike block that has intrinsic tension in its branches. The second component is a linear spacer which links the blocks in a particular way to focus the branch tension to the spacer. Figure 1 shows one of the simplest examples of the tension amplifier, a pom-pom macromolecule with two z -arm starlike brushes connected with a linear spacer. The tension in the brush arms is typically below 1 pN. By linking molecular stars, the individual tensions from z arms get focused to the single spacer leading to z -fold amplification of the spacer tension.

Such pom-poms can be synthesized starting from a linear precursor consisting of m Kuhn segments of length b each and two branching centers AB_{p-1} at its ends (Fig. 2). This is followed by reacting AB_{p-1} monomers to each of $p-1$ reacting groups B (diverging polymerization [15,16]). This step is repeated $a-1$ times, resulting in a dual-core dendrimer with $2(p-1)^a$ end groups. Finally, $z = (p-1)^a$ linear arms are grown from each dendritic core. Since the tension in the arms decreases with distance from the branching centers, these arms should grow without significant steric hindrance, as long as the spacer length is larger than the diameter of the dendrimer. The grown arms repel each other and stretch the spacer. Using scaling approach, we will show that pom-pom architecture enables amplification of tension from the pN range in its arms to nN forces in the spacer.

Star

Linear chains in a z -arm polymer star are under tension. In good and θ solvents, this tension is determined by osmotic repulsion between extended arms [17]. At θ temperature, the second virial coefficient is zero; however, the net interaction is repulsive due to the positive third virial coefficient [18]. The average distance between monomers of neighboring arms (correlation length ξ) linearly increases with distance r from the center of the star as

$$\xi \simeq r/\sqrt{z}. \quad (1)$$

We drop numerical coefficients on the order of unity keeping our discussion on the scaling level. The osmotic repulsion leads to local tension in each arm as

$$f_{\text{arm}} \simeq kT/\xi \simeq kT\sqrt{z}/r \text{ for } r > R_c \simeq b\sqrt{z} \quad (\text{solvent}), \quad (2)$$

where R_c is the smallest radius of the dendrimer core for a star with z arms. The highest tension in the arms is achieved at the surface of the core ($r = R_c$) as

$$f_0 \simeq kT/b \quad (3)$$

which is $\simeq 4$ pN for a typical Kuhn monomer length $b \simeq 1$ nm.

It is less evident that the densely grafted arms are also stretched in poor solvents and even in a melt state, where the arms can overlap [19–21]. In this case, their extension is caused by constrained packing of z arms into a small volume. For a “dry” star (melt), the arm tension changes with r as

$$f_{\text{arm}} \simeq kTzb/r^2 \text{ for } r > R_c \text{ (melt)}. \quad (4)$$

Note that the maximum tension $f_0 \simeq kTb \simeq 4$ pN is the same as in the case of a “wet” star [Eq. (3)].

Pom-Pom

Here we use the scaling model of star polymers to demonstrate the basic principles of bond-tension amplification by focusing the tension from individual branches to a particular polymer strand within a branched macromolecule. If two z -arm stars are pushed together, there is a repulsive force due to steric crowding of the arms. This repulsion is balanced by linking the stars with a spacer of length d . The tension in the spacer can be calculated from the difference between the free energies of $2z$ -arm star and two z -arm stars. For example, the energy difference in solution can be written as

$\Delta F \simeq F_{2z} - 2F_z \simeq kT(2z) \sqrt{2z} \ln(R_{2z}/r) - 2kTz \sqrt{z} \ln(R_z/r)$, where R_z (and R_{2z}) is the radius of a z -arm (and $2z$ -arm) star and r is the radius of the unperturbed regions of each star [17]. This gives the spacer tension $f = -\partial(\Delta F)/\partial r \simeq f_0 z^{3/2} b/d$, which can be interpreted as a sum of tensions in z individual arms measured at a distance $r \simeq d$. Using Eqs. (2) and (4), one calculates the tension as

$$f \simeq f_0 z^{3/2} b/d \text{ (solvent)}, \quad (5a)$$

$$f \simeq f_0 z^2 b^2/d^2 \text{ (melt)}. \quad (5b)$$

A short spacer becomes fully stretched ($d = bm$) if its tension $f_{\text{sp}} > f_0$ [Eq. (3)]. In this case, the tension is given by Eq. (5):

$$f_{\text{sp}} \simeq f_0 z^{3/2}/m \text{ for } z^{1/2} < m < z^{3/2} \text{ (solvent)}, \quad (6a)$$

$$f_{\text{sp}} \simeq f_0 z^2/m^2 \text{ for } z^{1/2} < m < z \text{ (melt)}. \quad (6b)$$

Here, the lower limit for m is given by the radius of the dendrimer cores (Fig. 1), i.e., $m^2 \sim R_c^2 \sim z$, while the upper limit of m is given by the lower limit of the spacer tension ($f_{\text{sp}} \simeq f_0$) at its full extension. For short spacers ($m \simeq z^{1/2}$), the tension is on the order of zf_0 . For example, 7th-generation dendrimers with a branching functionality $p = 3$ and $z = 512$ arms [15,16] induce tension in the spacer of about 512×4 pN $\simeq 2$ nN, which is close to the strength of covalent bonds [1]. Note that the dendrimer radius should be 6.5 nm to accommodate 512 arms at a grafting density of 1 chain/nm² [22,23], which is consistent with the radius of a typical 7th generation dendrimers. The tension of longer spacers with $m > z^{1/2}$ is lower; however, it can be fine-tuned by adjusting the quality of the solvent between the two limits, defined in Eq. (6). Here, the melt state corresponds to the limiting poor solvent condition, called nonsolvent.

Figure 3 shows the equilibrium tension f_{sp} as a function of the spacer length in different solvents. In the high tension range ($f_{sp} > f_0$), the bond tension in the fully extended spacer ($d = bm$) is given by Eq. (6). The equilibrium size of a longer spacer (which is not fully extended) is obtained by balancing the tensile force [Eq. (5)] by the chain elasticity $f_{el} = kTd/(b^2m) = f_0d/(bm)$ as

$$d \simeq bm^{1/2}z^{3/4} \text{ for } m > z^{3/2} \quad (\theta\text{-solvent})$$

$$d \simeq bm^{1/3}z^{2/3} \text{ for } m > z \quad (\text{melt}).$$

The corresponding tension can be written as

$$f_{sp} \simeq f_0z^{3/4}/m^{1/2} \text{ for } m > z^{3/2} \quad (\theta\text{-solvent}), \quad (7a)$$

$$f_{sp} \simeq f_0z^{2/3}/m^{2/3} \text{ for } m > z \quad (\text{melt}). \quad (7b)$$

The crossover between the two limiting solvent conditions in Eqs. (6) and (7) can be described by introducing the excluded volume parameter ν , on the order of $-b^3$ in a nonsolvent (melt) and $\nu = 0$ in a θ -solvent [18]. For intermediate values of $\nu = b^3\tau$ ($-1 < \tau < 1$), the tension in the spacer follows the θ behavior until the correlation length in the star at $r = d$ [Eq. (1)] becomes larger than the size of the thermal blob $b/|\tau|$ [18]. In longer spacers, the tension follows the nonsolvent (melt) behavior and depends on the parameter of the solvent quality τ (middle lines in Fig. 3).

Different regimes of tension amplification in solvents of different quality are presented in Fig. 4. Part of the diagram to the left of the thick solid line corresponds to a fully extended spacer (regimes θS and PS) with $f_{sp} > f_0$, while the right part of this diagram corresponds to a weakly extended spacer (regimes θW and PW). Along the thin line in Fig. 4, the size of the thermal blob $b/|\tau|$ is on the order of correlation length d/\sqrt{z} at the length scale of the spacer [Eq. (1)]. This line separates θ -solvent regimes (θS and θW) from poor solvent regimes (PS and PW). The upper part of the diagram (regimes θS and θW) corresponds to θ solvent with the spacer tension given by Eqs. (6a) and (7a), see line *A* in Fig. 3. The nonsolvent ($\tau = -1$) regime corresponds to the bottom boundary of the diagram, where the tension is given by Eqs. (6b) and (7b), see the lowest line (thin solid line *D*) in Fig. 3.

In moderately poor solvent with $-1 < \tau < -z^{-1}$, the crossover between θ -like (regime θS) and poor-solvent-like (regime PS) behavior occurs in the lower part of the diagram in Fig. 4 (e.g., along the dotted line *C*). The tension along line *C* is

$$f_{sp} \simeq f_0z^{3/2}/m, \text{ for } z^{1/2} < m < z^{1/2}|\tau|^{-1} \quad (8a)$$

$$f_{sp} \simeq f_0z^2/(|\tau|m^2), \text{ for } z^{1/2}|\tau|^{-1} < m < z|\tau|^{-1/2} \quad (8b)$$

$$f_{\text{sp}} \simeq f_0 z^{2/3} |\tau|^{-1/3} m^{-2/3}, \text{ for } z |\tau|^{-1/2} < m < N/z. \quad (8c)$$

as shown by the dashed curve C in Fig. 3. Closer to the θ point with $-z^{-1} < \tau < 0$ (dashed line B in Fig. 4) the tension shows the θ -like behavior [Eq. (6a)] for a strongly stretched spacer (regime θS) with $z^{1/2} < m < z^{3/2}$ and continues into the Gaussian zone for a weakly stretched spacer (regime θW), following Eq. (7a) for $z^{3/2} < m < z^{-1/2} |\tau|^{-2}$. The tension of longer spacers (regime PW) is given by the poor solvent expression [Eq. (8c)] for $z^{-1/2} |\tau|^{-2} < m < N/z$, see the dashed line B in Fig. 3.

One of the important findings of this work is that the tension in a spacer can be fine-tuned by adjusting the quality of the solvent. For example, one can start with the spacer, consisting of $z^{1/2} < m < z$ Kuhn segments in a nonsolvent (melt) state with the tension in the spacer given by Eq. (6b). As the solvent quality improves (arrow in Fig. 3) the tension in the spacer increases as $|\tau|^{-1}$ [Eq. (8b)] and saturates at the θ -solvent value of f_{sp} [Eq. (8a)] for solvents with $|\tau| \lesssim z^{1/2}/m$. The maximum solvent-induced change in tension by a factor of $z^{1/2}$ is predicted for a spacer with $m = z$. In the case of 7th-generation dendrimer (considered above), the spacer tension increases from $f_0 \simeq 4$ pN (in a melt with $\tau \simeq -1$) to $f_{\text{sp}} \simeq \sqrt{z} f_0 \simeq 0.1 \text{ nN}$ (at nearly θ temperature with $|\tau| \lesssim 0.03$).

Surprisingly, improving the solvent quality above the θ point ($\tau > 0$) does not increase the tension in the spacer. For a fully extended spacer ($z^{1/2} < m < z^{3/2}$), the correlation length ξ at the fixed distance $r = bm$ from the branching center is determined by the number of monomers, m , in the spacer $\xi \simeq bm / \sqrt{z}$ [Eq. (1)] independent on solvent quality. In the case of longer spacers ($m > z^{-1/2} \tau^{-2}$), the behavior is even more surprising since the tension decreases with the solvent quality as

$$f_{\text{sp}} \simeq f_0 z^{7/10} \tau^{-1/5} m^{-3/5}, \quad (\text{good solvent}). \quad (9)$$

This softening is due to the partial swelling of the spacer and the resulting change of spacer elasticity from the Gaussian to nonlinear regime.

Another important result is that the tension amplification is independent of the number of monomers N in the arms and their polydispersity at $N > m^3/z$ for fully extended spacers with $m < z$ and at $N > mz$ for $m > z$. This underscores the origin of the tension due to local crowding of the $2z$ star-arms at a distance $r \simeq mb$. At $r < mb$, the arms maintain unperturbed conformation of single stars. At larger distances ($r > mb$), the steric repulsion rapidly decays due to the spherical shape of the stars resulting in logarithmic distance dependence of the energy.

In this Letter, we demonstrate that one can design a macromolecule which generates high bond tension (on the order of nN) in solution without applying an external force. The design strategy is based on linking multiple branches in such a way that weak (pN) tension in individual branches is focused and amplified to the nN range where covalent bonds fundamentally change their electronic structure and may eventually break. In addition to pom-poms, there are other types of branched architectures that allow tension amplification.

For example, in cylindrically shaped molecular brushes, the tension from densely grafted side chains is focused to the backbone leading to significant tension increase which depends on the grafting density and the solvent quality [24]. The tension in the backbone is minimal in a nonsolvent with $\tau = -1$ (melt), $f_{\text{sp}} \simeq f_0$, and increases with solvent quality, reaching the value $f_0 N^{1/3}$ in a θ -solvent ($\tau = 0$) and $f_0 N^{3/8}$ in an athermal solvent ($\tau = 1$). Unlike pom-poms, the tension in the brush backbone depends on the side-chain length N .

Acknowledgments

We would like to acknowledge financial support of National Science Foundation under Grants No. CHE-0616925 (M. R.), No. DMR-0606086 (S. S. S.), and No. CBET-0609087 (M. R. & S. S. S.), National Institutes of Health under Grant No. 1-R01-HL0775486A (M. R.), and Petroleum Research Fund under Grant No. 46204-AC7 (S. S. S.). We are grateful to E. B. Zhulina for very stimulating discussions.

References

1. Beyer MK, Clausen-Shaumann M. *Chem. Rev.* 2005; 105:2921. [PubMed: 16092823]
2. Discher DE, Janmey P, Wang Y-L. *Science.* 2005; 310:1139. [PubMed: 16293750]
3. Evans EA, Calderwood DA. *Science.* 2007; 316:1148. [PubMed: 17525329]
4. Wiita AP, Ainaravaru SRK, Huang HH, Fernandez JM. *Proc. Natl. Acad. Sci. U.S.A.* 2006; 103:7222. [PubMed: 16645035]
5. Mehta AD, Rief M, Spudich JA, Smith DA, Simmons RM. *Science.* 1999; 283:1689. [PubMed: 10073927]
6. Janshoff A, Neitzert M, Oberdorfer Y, Fuchs H. *Angew. Chem., Int. Ed.* 2000; 39:3212.
7. Bustamante C, Keller D, Oster G. *Acc. Chem. Res.* 2001; 34:412. [PubMed: 11412078]
8. Grandbois M, Beyer M, Rief M, Clausen-Schaumann H, Gaub HE. *Science.* 1999; 283:1727. [PubMed: 10073936]
9. Harrington RE, Zimm BH. *J. Phys. Chem.* 1965; 69:161.
10. Odell JA, Muller AJ, Narh KA, Keller A. *Macromolecules.* 1990; 23:3092.
11. Watson WF. *Makromol. Chem.* 1959; 34:240.
12. Zhurkov SN, Korsukov VE. *J. Polym. Sci., Polym. Phys. Ed.* 1974; 12:385.
13. Hickenboth CR, Moore JS, White SR, Scottos NR, Baudry J, Wilson SR. *Nature (London).* 2007; 446:423. [PubMed: 17377579]
14. Sheiko SS, et al. *Nature (London).* 2006; 440:191. [PubMed: 16525468]
15. Tomalia DA, Naylor AM, Goddard WA. *Angew. Chem., Int. Ed. Engl.* 1990; 29:138.
16. de Brabander-van den Berg EMM, Meijer EW. *Angew. Chem., Int. Ed. Engl.* 1993; 32:1308.
17. Daoud M, Cotton JP. *J. Phys. (Paris).* 1982; 43:531.
18. Rubinstein, M.; Colby, RH. *Polymer Physics.* Oxford, UK: Oxford University Press; 2003.
19. Zhulina EB, Birshtein TM. *Polym. Sci. USSR.* 1985; 27:570.
20. Birshtein TM, Zhulina EB. *Polymer.* 1989; 30:170.
21. Semenov AN. *Sov. Phys. JETP.* 1985; 61:733.
22. Tsujii, Y.; Ohno, K.; Yamamoto, S.; Goto, A.; Fukuda, T. *Advances in Polymer Science.* Vol. 197. Berlin: Springer; 2006. *Surface-Initiated Polymerization I*; p. 1
23. Brittain WJ, Minko S. *J. Polym. Sci. A.* 2007; 45:3505.
24. Panyukov S, Zhulina EB, Sheiko SS, Randal G, Brock J, Rubinstein M. *J. Phys. Chem. B.* 2009; 113:3750. [PubMed: 19673133]

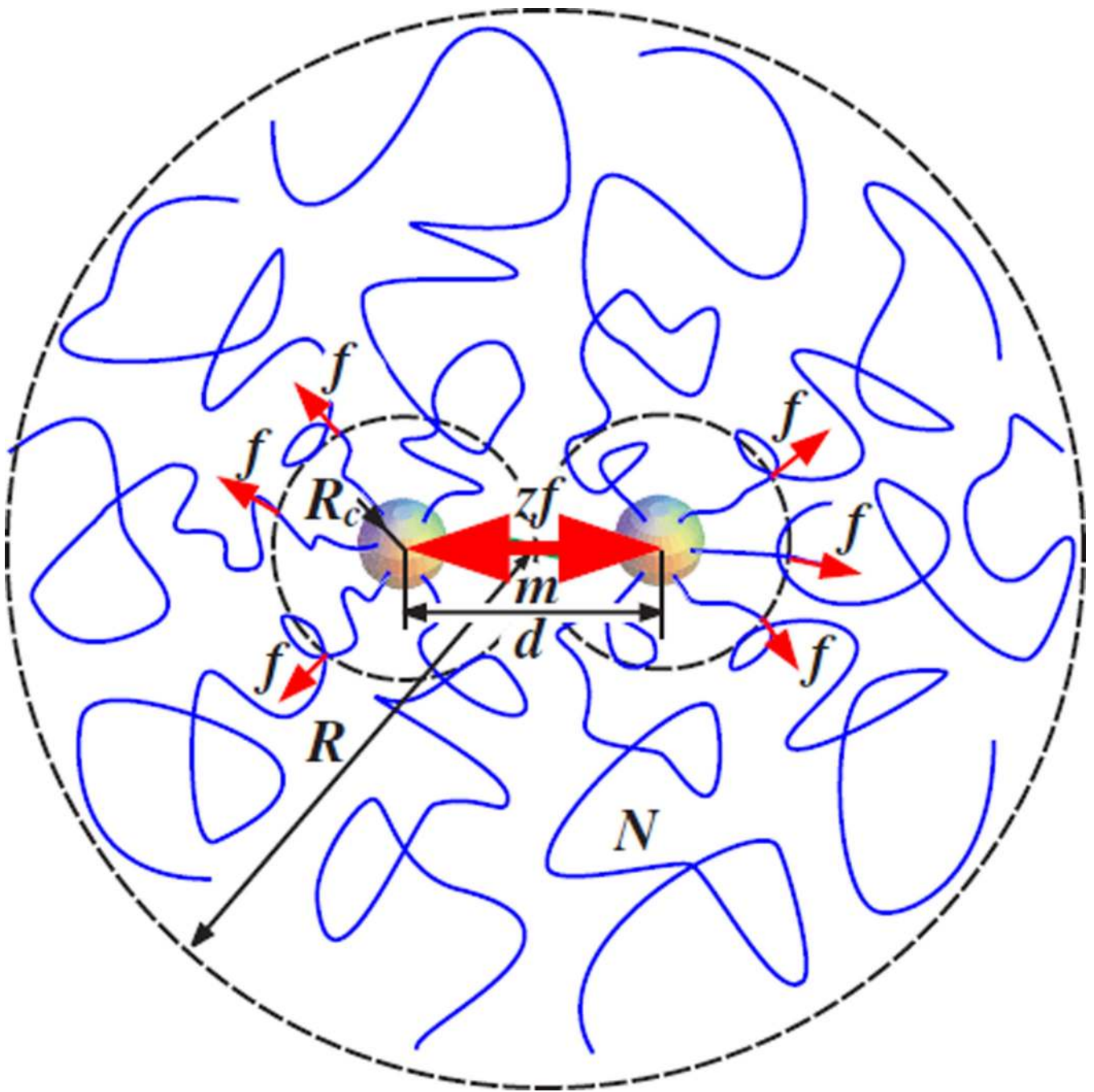


FIG. 1. (color online). Architecture of a pom-pom macromolecule including a dense (solid) branching core of radius R_c , a region ($R_c < r < d$) of unperturbed star arms, and the corona of $2z$ arms whose conformation is perturbed by linking (pushing) together two z -arm stars.

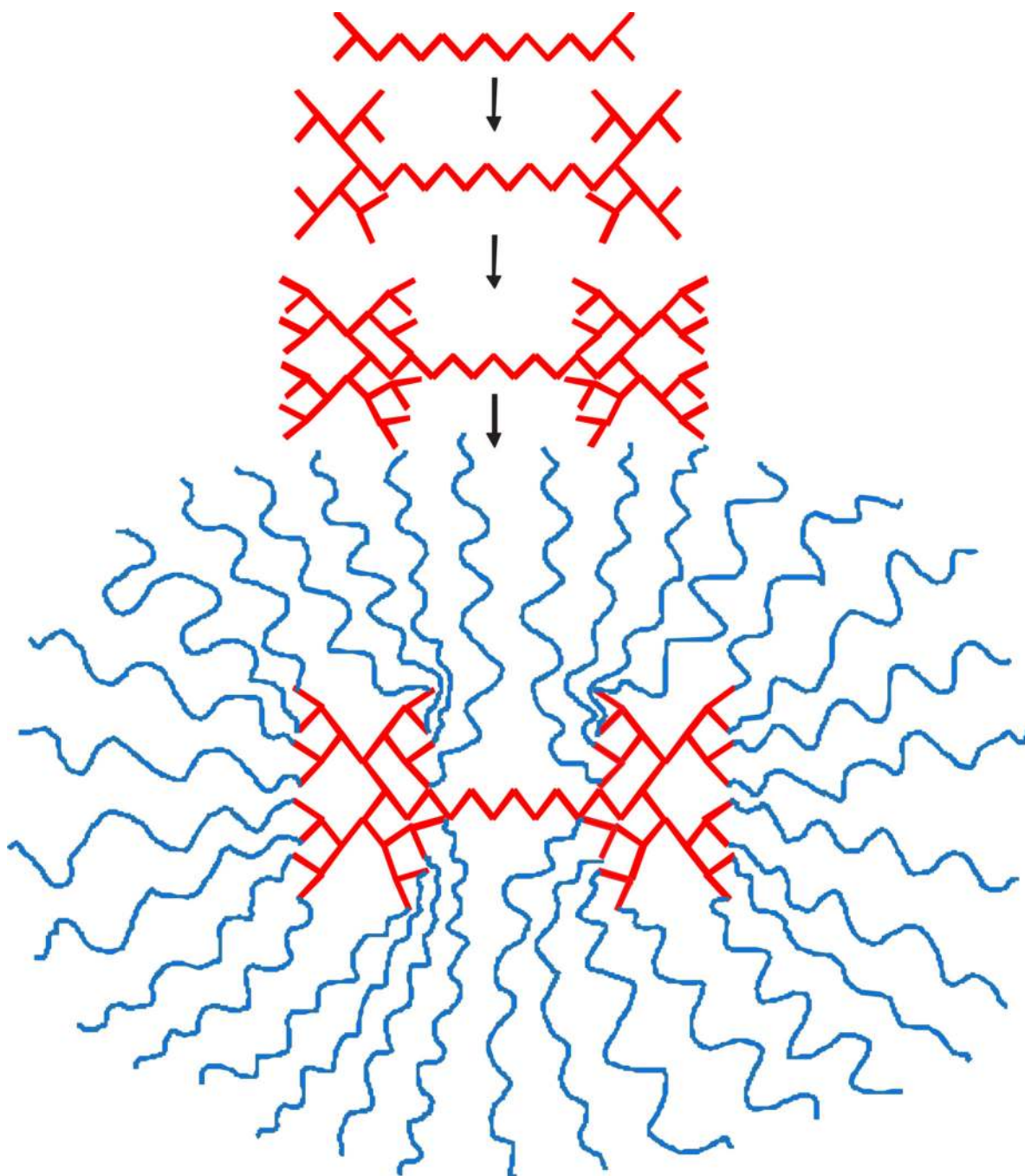


FIG. 2. (color online). Strategy for synthesizing pom-pom macromolecules which includes three major steps: (i) synthesizing a linear linker endcapped with branching functionalities, (ii) introducing z branches with reactive end groups, and (iii) growing z arms from these groups.

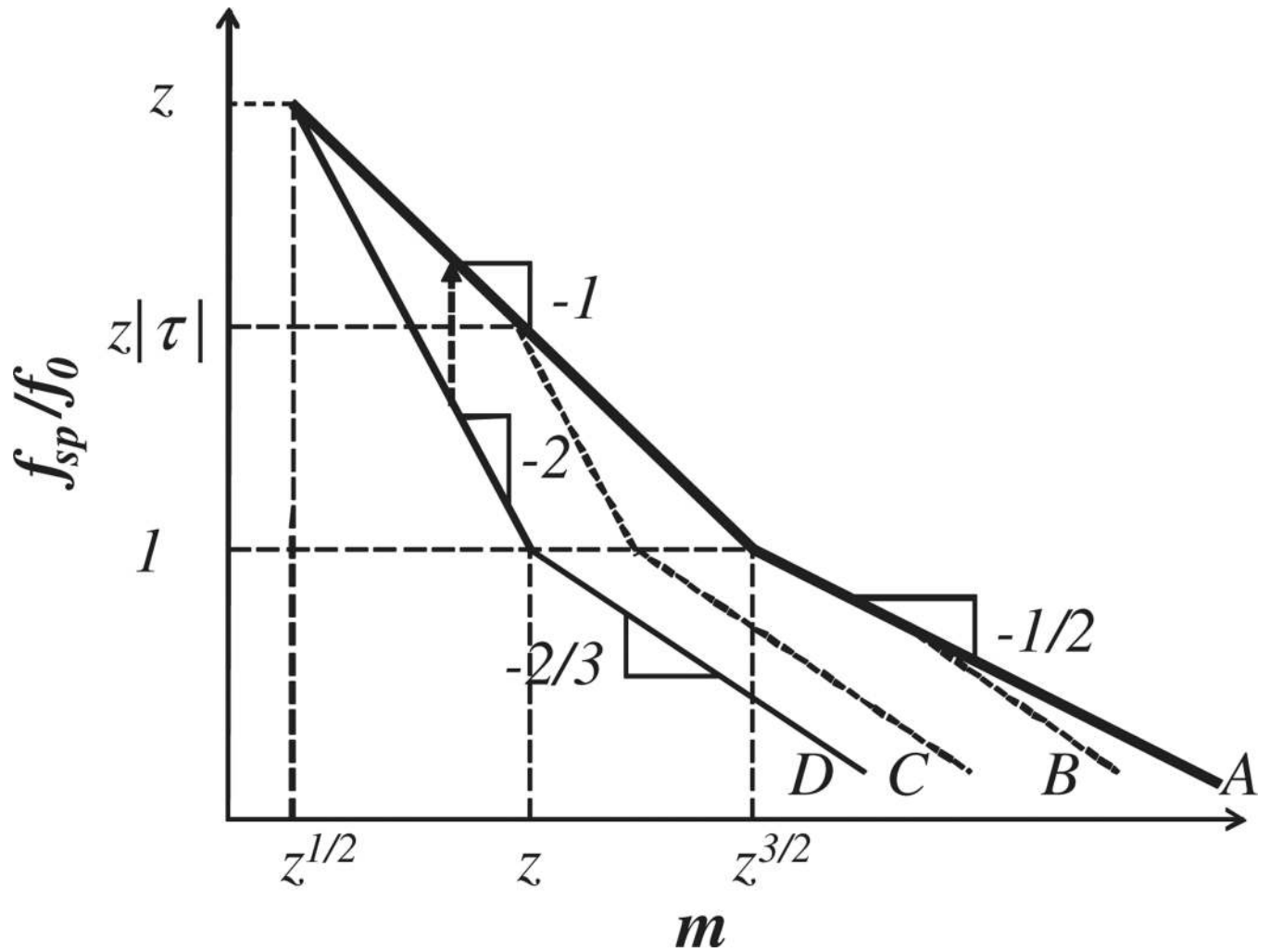


FIG. 3. Log-log plot of tension f_{sp} in a spacer with m Kuhn segments for pom-pom in different solvents. Upper curve— θ -solvent, middle curves—poor solvent; lower curve—melt condition.

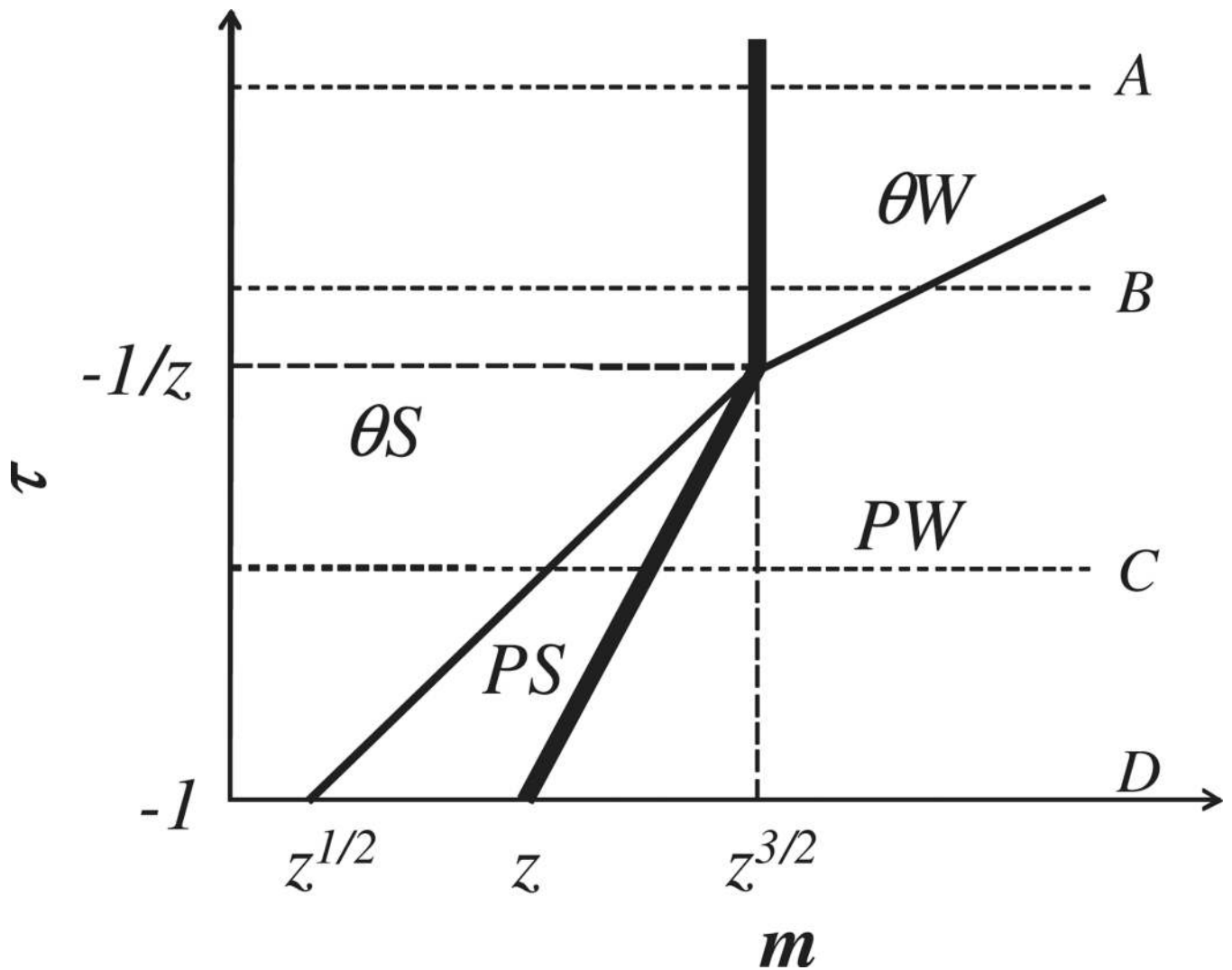


FIG. 4. Diagram of states of a pom-pom in a poor and theta (θ) solvents. The four regimes depicted in the diagram are θ solvent for arms with strongly (θS) and weakly (θW) stretched spacer as well as poor solvent for arms with strongly (PS) and weakly (PW) stretched spacer. The boundary between strongly and weakly stretched spacer (thick line in the diagram) is given by the fully extended chain ($d \simeq bN$). The logarithmic axes are $\ln(m)$ and $-\ln|\tau|$.